Interaction of Sapphyrin with Phosphorylated Species of Biological Interest

Brent L. Iverson,* Kevin Shreder, Vladimír Král, Petra Sansom, Vincent Lynch, and Jonathan L. Sessler*

Contribution from the Department of Chemistry and Biochemistry, University of Texas, Austin, Texas 78712

Received August 28, 1995[⊗]

Abstract: A model for the interaction of the water-soluble sapphyrin derivative **1** with a variety of nucleic acid species is presented. Three modes of interaction are described: The first mode, seen with all the nucleic acid species, is that of "phosphate chelation". This mode is exemplified by a solid state structure of the complex formed between the monobasic form of cAMP and the sapphyrin species $[2H\cdot\mathbf{2}]^{2+}$. It involves the specific chelation of the oxyanion of a phosphorylated nucleotide or nucleic acid species with the protonated core of sapphyrin *via* Coulombic interactions that include H-bonding interactions. Spectroscopically, this interaction is characterized by a visible absorption at 422 nm and corresponds to complexes formed between the dimeric form of **1** and phosphorylated nucleotides. In the case of double-stranded DNA, this mode of binding shows a preference for the more flexible copolymer $[poly(dA\text{-}dT)]_2$ over $[poly(dG\text{-}dC)]_2$. The second mode involves a hydrophobic interaction with the nucleobases present in both monomeric and single-stranded polymeric nucleotides. Spectroscopically, this nucleotide-dependent interaction is characterized by the absorption of the monomeric species of **1** at *ca.* 450 nm. The third mode involves the highly ordered aggregation of **1** on the surface of certain double-stranded, helical nucleic acids at low phosphate ester to sapphyrin (P/S) ratios and is templated by the higher order structure of these nucleic acid polymers. Spectroscopically, this mode is characterized by a visible absorption at *ca.* 400 nm and a large, conservative induced CD signal for **1**.

Introduction

Nucleotides and nucleic acids are essential constituents of a variety of biological structures and mechanisms. They play a key role in a wealth of critical processes ranging from information processing to energy storage and transduction.[1] As a result, Nature has developed a variety of clever and highly specific methods to manipulate the phosphate anion and its derivatives. For example, studies by Quiocho *et al.* have shown that phosphate-binding protein, through precisely architectured hydrogen-bonding interactions, can distinguish between phosphate and sulfate anions with a greater than five order of magnitude preference.[2] This exquisite specificity highlights the importance that the recognition of phosphate and phosphorylated species can play in biological systems.

In recent years considerable effort has been devoted to the development of small molecules capable of the specific recognition and transport[3] of phosphate and phosphate-bearing entities. Approaches taken have been based on a variety of motifs, including ones based on the naturally occurring guanidinium group[3f,4] and expanded porphyrins.[5,6] As part of an effort to develop the latter species as phosphate recognition "tools", we became interested in determining how the sapphyrins (e.g., **1**−**3**; Figure 1), a class of pentapyrrolic aromatic macrocycle,[7] would interact with mononucleotides and nucleic acids.

Previously, we reported the ability of sapphyrins to bind to the anionic phosphodiester backbone of DNA *via* a novel interaction that we call "phosphate chelation".[8] In this paper we elaborate on "phosphate chelation" as a mode of binding to nucleotides and nucleic acids and discuss how the aggregation state of sapphyrin is influenced by anion binding in aqueous media. Specifically, we show that the monoprotonated form of sapphyrin can exist in three limiting forms, namely as a monomer, a dimer, or a non-covalent, aggregated polymer. These forms can interact with nucleotides and nucleic acids not only *via* phosphate chelation but also *via* two other distinct modes that can be distinguished by the state of aggregation of the sapphyrin macrocycle. We also report the results of control studies carried out with the porphyrin system **4** (Figure 1).

Experimental Section

Materials. The 3′:5′-cyclic monophosphate nucleotides (cXMP, where X = A, C, G, or T), single-stranded calf thymus DNA (ssDNA), and double-stranded calf thymus DNA (type XV) (dsDNA) were purchased from Sigma. Poly(dA-dT)·poly(dA-dT) ($[poly(dA\text{-}dT)]_2$) and poly(dG-dC)·poly(dG-dC) ($[poly(dG\text{-}dC)]_2$) were purchased from Pharmacia Biotech. DsDNA and ssDNA were dialyzed exhaustively against 5 mM PIPES, pH 7.0. SsDNA was heated to 100 °C for 15 min and

[⊗] Abstract published in *Advance ACS Abstracts,* February 1, 1996.

(1) Adams, R. L. P.; Knowler, J. T.; Leader, D. P., Eds. *The Biochemistry of the Nucleic Acids*, 10th ed.; Chapman and Hall: New York, 1986.

(2) Luecke, H.; Quiocho, F. A. *Nature* **1990**, *347*, 402−406.

(3) (a) Tabushi, I.; Kobuke, Y.; Imuta, J. *J. Am. Chem. Soc.* **1980**, *102*, 1744−1745. (b) Tabushi, I.; Kobuke, Y.; Imuta, J. *J. Am. Chem. Soc.* **1981**, *103*, 6152−6157. (c) Furuta, H.; Cyr, M. J.; Sessler, J. L. *J. Am. Chem. Soc.* **1991**, *113*, 6677−6678. (d) Tingyu, L.; Diederich, F. *J. Org. Chem.* **1992**, *57*, 3449−3454. (e) Kuroda, Y.; Hatakeyama, H.; Seshimo, H.; Ogashi, H. *Supramol. Chem.* **1994**, *3*, 267−271. (f) Andreu, C.; Galán, A.; Kobiro, K.; de Mendoza, J.; Park, T. K.; Rebek, J., Jr.; Salmerón, A.; Usman, N. *J. Am. Chem. Soc.* **1994**, *116*, 5501−5502.

(4) (a) Dietrich, B.; Fyles, D. L.; Fyles, T. M.; Lehn, J.-M. *Helv. Chim. Acta* **1979**, *62*, 2763−2787. (b) Hannon, C. L.; Anslyn, E. V. The Guanidinium Group: Its Biological Role and Synthetic Analogs. In *Bioorganic Chemistry Frontiers;* Dugas, H., Schmidtchen, F. P., Eds.; Springer: Heidelberg, 1993; Vol. 3, pp 193−255.

(5) Sessler, J. L.; Furuta, H.; Král, V. *Supramol. Chem.* **1993**, *1*, 209−220.

(6) (a) Furuta, H.; Cyr, M. J.; Sessler, J. L. *J. Am. Chem. Soc.* **1991**, *113*, 6677−6678. (b) Iverson, B. L.; Shreder, K.; Král, V. K.; Smith, D. A.; Smith, J.; Sessler, J. L. *Pure Appl. Chem.* **1994**, *66*, 845−850. (c) Iverson, B. L.; Thomas, R. E.; Král, V. K.; Sessler, J. L. *J. Am. Chem. Soc.* **1994**, *116*, 2663−2664.

(7) (a) Sessler, J. L.; Burrell, A. K. *Top. Curr. Chem.* **1991**, *161*, 177−273. (b) Sessler, J. L.; Cyr, M. J.; Burrell, A. K. *Synlett* **1991**, 127−134.

(8) Iverson, B. L.; Shreder, K.; Král, V. K.; Sessler, J. L. *J. Am. Chem. Soc.* **1993**, *115*, 11022−11023.

0002-7863/96/1518-1608$12.00/0

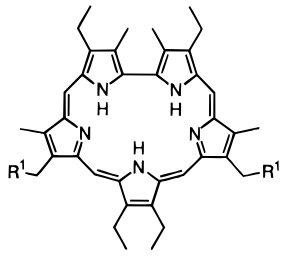

1 $R^1 = CH_2CON(CH_2CH_2OH)_2$
2 $R^1 = CH_2CH_2OH$
3 $R^1 = CH_3$

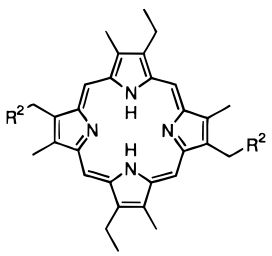

4 $R^2 = CON(CH_2CH_2OH)_2$

Figure 1. Structures of the macrocycles used in this study.

then quickly cooled in ice prior to use. The concentration of DNA-phosphate was determined spectrophotometrically using A_{260} values provided by the manufacturers. The syntheses of the sapphyrin derivatives **1** and **2** and the porphyrin **4** are described in the preceding paper.[9]

Methods. ^{31}P NMR spectra were recorded on a Nicolet NT-360 spectrometer (81 MHz) using phosphoric acid as the external reference. The cyclic 3′−5′ nucleotide monophosphates (5 mM) were dissolved in deuterium oxide−methanol (1:2) and the spectrum recorded in each case. Then, 1 molar equiv of sapphyrin **1** was added and the spectrum re-recorded. In the case of cAMP and cCMP, studies were made using the free-acid form of the nucleotide and the free-base form of **1**. For cTMP and cGMP the sodium salt of the nucleotide and the monohydrochloride adduct of **1** were employed. Relevant data, derived from an average of two measurements (error ≤5%), are shown in Table 1.

UV−visible spectra were taken with a DU 600 spectrophotometer (Beckman Instruments, Inc., Fullerton, CA). CD spectra were obtained using a Jasco J-600 spectropolarimeter. Steady-state fluorescence spectra were recorded with a Perkin-Elmer LS5 spectrofluoremeter. Fluorescence spectra were obtained using excitation at 415 nm and were integrated between 600 and 800 nm. The resulting spectra were corrected for both the photomultiplier response and changes in the absorbance at the excitation wavelength.

All titrations were conducted at a fixed 3 μM concentration of sapphyrin **1** in 5 mM PIPES, pH 7.0. This concentration yielded a Soret-like absorption with a λ_{max} of 409 nm ($\epsilon_{409} = 140\,000\ M^{-1}\cdot cm^{-1}$). Concentrated solution of nucleotides and nucleic acids used in the titrations were prepared using a 3 μM solution of **1** in 5 mM PIPES, pH 7.0. As a result, the concentration of sapphyrin **1** remained unchanged throughout the course of the titration allowing spectroscopic differences to be monitored accurately as the relative sapphyrin-to-phosphate ratios varied. The mixtures obtained after adding each aliquot of nucleic acid were allowed to equilibrate for up to 15 min prior to recording the spectrum. This longer time period was used to allow time for equilibration between the putative modes of binding that involved "phosphate chelation" and aggregation.

Viscometric studies were performed using a Cannon-Ubbelohde calibrated viscometer (Cannon Instrument Co., State College, Pennsylvania) according to the procedure of Cohen and Eisenberg.[10] All titrations were made in 5 mM PIPES, pH 7.0, using a fixed concentration of dsDNA (in base pairs) of 1.5×10^{-4} M. Flow times were measured by hand with a stopwatch accurate to 0.1 s. A total of five time readings were taken and averaged for each datum point. Reduced intrinsic viscosity was plotted as a function of the ratio of sapphyrin to DNA base pairs between 0 and 0.12. Problems with coprecipitation of **1** and dsDNA were avoided by the slow, dropwise addition of a 2× stock solution of sapphyrin into an equal volume of a 2× solution of dsDNA with gentle vortexing. The resulting solutions were transparent and no green fibers, indicative of coprecipitation, were observed after ultracentrifugation.

X-ray Experimental Procedure. Crystals of $(C_{42}H_{55}N_5O_2^{2+})(C_{10}H_{14}N_5O_6P^-)Cl^-(C_4H_{10}O)$ were grown as dark, almost black plates by allowing diethyl ether as the volatile phase to diffuse slowly into a solution of $[2H\cdot\mathbf{2}]^{2+}\cdot cAMP^-\cdot Cl^-$ in 4:1 MeOH/$CHCl_3$. The original mixed salt was obtained by washing a solution of $[2H\cdot\mathbf{2}]^{2+}\cdot 2Cl^-$ in $CHCl_3$ with an aqueous solution of cAMP. The data crystal was a plate of approximate dimensions 0.14 × 0.34 × 0.34 mm. The data were collected at 183 K on a Nicolet P3 diffractometer, equipped with a Nicolet LT-2 low-temperature device and using a graphite monochromator with Mo Kα radiation ($\lambda = 0.71073$ Å). Details of crystal data, data collection and structure refinement are provided in the supporting information. Final refinement gave a Flack *x* parameter of 0.09(16).[11]

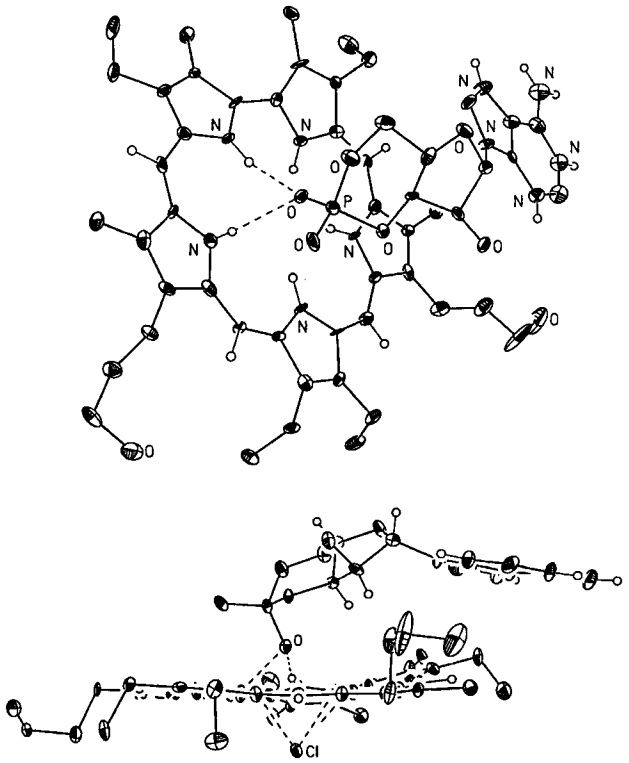

Figure 2. Two views, showing selected heteroatoms of the solid-state complex formed between monobasic cAMP, chloride anion, and $[2H\cdot\mathbf{2}]^{2+}$. The top view shows the details of the interaction between monobasic cAMP and $[2H\cdot\mathbf{2}]^{2+}$. The bottom view shows an edge-on view of the complex. The bound oxyanion of cAMP and the chloride anion are found 1.376 and 1.820 Å, respectively, above the root-mean-square plane of the pyrrolic nitrogens. The phosphorus atom is 2.667 Å from this same plane.

Results and Discussion

Interaction with Mononucleotides in the Solid State. Previous studies,[5,12] including the paper prior to this one,[9] have provided solid-state X-ray diffraction structures of [2H·sapphyrin]$^{2+}$ cations chelated to the monobasic forms of phosphoric, phenyl phosphoric, and diphenyl phosphoric acid. Taken together, these structures provide evidence that, at least in the solid state, phosphate anion complexation takes place *via* Coulombic attractive forces that include H-bonding interactions with the cationic, macrocyclic core of sapphyrin. These findings led us to coin the term "phosphate chelation" and inspired us to test whether sapphyrins could also bind with either nucleotides or DNA.

As a first step toward testing this postulate, X-ray quality crystals of the mixed chloride/monobasic cAMP salt of $[2H\cdot\mathbf{2}]^{2+}$ were grown. They yielded the structure shown in Figure 2. This structure bears a chimeric resemblance to that of the dichloride complex, phenyl phosphate complex, and diphenyl

(9) Král, V. K.; Shreder, K.; Furuta, H.; Lynch, V.; Sessler, J. L. *J. Am. Chem. Soc.* **1996**, *118*, 1595−1607.
(10) Cohen, G.; Eisenberg, H. *Biopolymers* **1969**, *8*, 45−49.
(11) Flack, H. D. *Acta Crystallogr.* **1983**, *A39*, 876−881.
(12) Sessler, J. L.; Cyr, M.; Furuta, H.; Král, V.; Mody, T.; Morishima, T.; Shionoya, M.; Weghorn, S. *Pure Appl. Chem.* **1993**, *65*, 393−398.

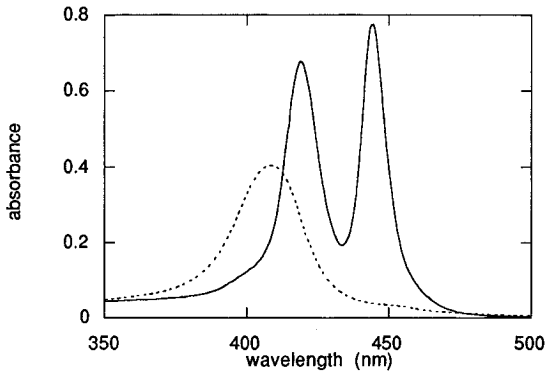

Figure 3. Visible spectra of 3 μM sapphyrin **1** in 5 mM PIPES, pH 7.0 (- - -), and in the presence of a 50% (v/v) solution of CH_3CN in 5 mM PIPES, pH 7.0 (—).

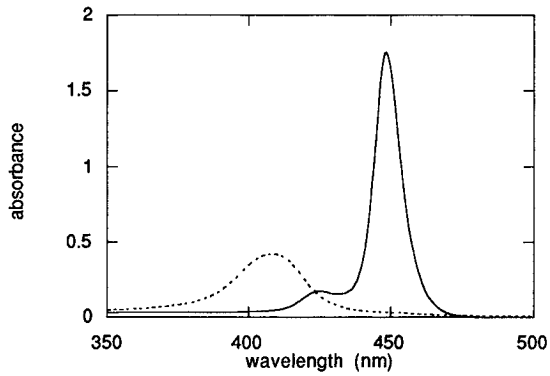

Figure 4. Visible spectra of 3 μM sapphyrin **1** in 5 mM PIPES, pH 7.0 (- - -), and in the presence of a 1% (w/w) SDS solution in 5 mM PIPES, pH 7.0 (—).

phosphate complexes of $[2H\cdot\text{sapphyrin}]^{2+}$ mentioned above: The anionic oxygen of $cAMP^-$ is held on the "top" of the structure within hydrogen bonding distance to two of the five pyrrolic hydrogens, whereas the chloride anion on the "bottom" half is held in place by the remaining three pyrrolic hydrogens. The relevant nitrogen-to-bound oxyanion distances are 2.897 Å (N4) and 2.737 Å (N5), values that are completely consistent with the kind of hydrogen-bonding interactions expected for "phosphate chelation".

Spectroscopic Assignments. To extend the above solid-state studies, UV−visible spectroscopy was used to probe the phosphate binding properties of sapphyrin. Previous studies[13] of organic soluble sapphyrins have served to identify two spectroscopically distinct states for the decaalkyl sapphyrin system $[2H\cdot\mathbf{3}]^{2+}\cdot 2Cl^-$. The first, with a λ_{max} of 456 nm, is observed in nonpolar, organic media (e.g., $CHCl_3$) or at low concentrations in polar organic solvents (e.g., CH_3CN and MeOH) and was assigned to the monomeric form. The second, with a λ_{max} of 422 nm, is observed at higher concentrations in polar organic media (e.g, CH_3CN and MeOH) and was assigned to the dimeric form. Recent findings consistent with this interpretation have indicated that a flexible, covalently-linked sapphyrin dimer exhibits two absorptions at 422 and 441 nm, indicative of the closed (dimeric) and extended ("bis-monomeric") forms, respectively.[14] As a result, spectral assignments for these two critical sapphyrin structures are considered secure.

In 5 mM PIPES, pH 7.0 (the conditions used throughout this study), the water-soluble sapphyrin **1** exhibits a green color, the result of a broad, Soret-like absorption at *ca.* 410 nm in the visible region. The addition of CH_3CN results in the appearance of two bands, one at *ca.* 420 nm ascribed to the dimeric form and another at *ca.* 450 nm assigned to the monomeric form (Figure 3). Distinct absorptions or composite absorptions of these two species can be observed depending on the mole fraction of CH_3CN used.[15] Adding sodium dodecyl sulfate (SDS; Figure 4) results in the monomerization of sapphyrin as the result of solubilization by the "greasy" ends of this detergent.[16] Here, in analogy to what is seen in organic solvents, the large absorption at *ca.* 450 nm observed in the presence of SDS can be assigned to the monomeric form of **1**.

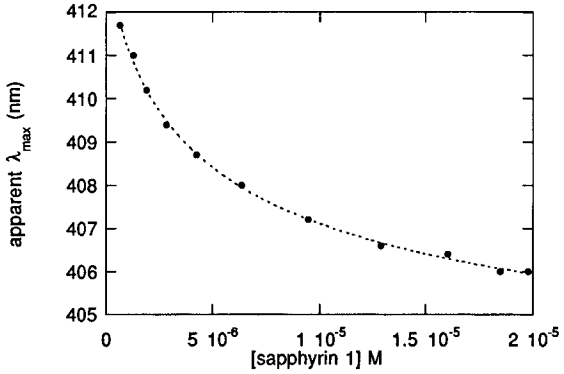

Figure 5. Change in the λ_{max} of 3 μM sapphyrin **1** as a function of its concentration in 5 mM PIPES, pH 7.0.

In order to assign the band at 410 nm, a dilution study was carried out over a concentration range of 1 to 20 × 10^{-6} M. As can be seen in Figure 5, the absorption maximum (λ_{max}) of **1** was observed to change significantly as a function of concentration. At lower concentrations, the λ_{max} redshifts; while at higher concentrations, it blueshifts. This behavior is, of course, consistent with aggregation. The observed shift in the λ_{max} reflects the presence of a continuum of equilibria involving the aggregated forms of **1** in solution. These range from highly aggregated states at higher concentrations of **1** to states of lesser aggregation at lower concentrations of **1**.

The above interpretations are by no means unique to the present sapphyrin system. A variety of chromophores, such as xanthene dyes[17] and acridine orange,[18] are known to undergo significant changes in the position of their λ_{max} as a function of their state of aggregation. *Importantly, the spectral shifts for **1** observed in this experiment indicate that the position of the* λ_{max} (or apparent λ_{max})[19] *is a useful indicator, in a qualitative sense, of the state of aggregation of **1**.* Because of the high degree of aggregation of **1** under aqueous, buffered conditions,

(13) Maiya, B. G.; Cyr, M.; Harriman, A.; Sessler, J. L. *J. Phys. Chem.* **1990**, *94*, 3597− 3601.

(14) Král, V.; Andrievsky, A.; Sessler, J. L. *J. Am. Chem. Soc.* **1995**, *117*, 2953−2954.

(15) When this experiment was repeated using various ratios (v/v) of CH_3CN: aqueous buffered solution at both pH 6.3 and 9.3 (5 mM bis-Tris propane·HCl), identical patterns of growth for this absorption at 444 nm were observed as a function of increasing CH_3CN. Because of the comparable behavior at these widely different pH values, we do not assign the absorption band at *ca.* 450 nm to a species associated with $[2H\cdot\mathbf{1}]^{2+}$, but rather to the monomeric form of $[H\cdot\mathbf{1}]^+$.

(16) Judy, M. M.; Matthews, J. L.; Newman, J. T.; Skiles, H. L.; Boriack, R. L.; Sessler, J. L.; Cyr, M.; Maiya, B. G.; Nichol, S. T. *Photochem. Photobiol.* **1991**, *53*, 101−107.

(17) Valdez-Aguilera, O.; Neckers, D. C. *Acc. Chem. Res.* **1989**, *22*, 171−177.

(18) Interestingly, the spectroscopic relationship between the state of aggregation and the λ_{max} of **1** resembles that previously proposed for acridine orange. In the case of acridine orange, the monomeric form absorbs at a higher wavelength than the dimer which, in turn, absorbs at higher wavelength than an extensively aggregated form. A similar effect is seen on the surface of polyanions. While we maintain that the underlying mode of DNA recognition for sapphyrin differs from that of acridine orange, we nonetheless recognize that the underlying photophysics for these two system are similar. See: Bradley, D. F.; Wolf, M. K. *Proc. Natl. Acad. Sci. U.S.A.* **1959**, *45*, 944−952, and references therein.

(19) The term "apparent λ_{max}" is used to indicate the observed λ_{max} of two or more overlapping absorption bands.

a fixed concentration of 3 μM for **1** was used in this study. This concentration represents the lowest one at which reliable spectroscopic data can be collected without resorting to inordinately long path lengths.

Previous work[9] has shown that the addition of phosphate anion or phosphorylated species to an aggregated form of sapphyrin initially leads to the "phosphate chelation" mode of binding (as judged from ^{31}P NMR) and a growing in of an absorption at *ca.* 450 nm. For example, the addition of phenylphosphate or phenyl phosphonate to an aggregated form of **1** under aqueous, buffered conditions[20] results in the disappearance of the characteristic absorption of this species at 403 nm and the appearance of an absorption band at 420 nm. This latter band was assigned to the dimeric, phosphate-bound species. Using the change in absorbance of this 420-nm band as a measure of binding, standard curve fitting procedures[20] yielded apparent K_a's of 300 and 310 M^{-1} for the binding of phenyl phosphate or phenylphosphonate to the dimeric form of **1**, respectively. Thus, the questions to be addressed in the context of the present study were whether the addition of phosphorylated species of biological interest leads to (1) spectroscopically distinct states and/or (2) the break up of the sapphyrin aggregates initially present in H_2O.

Interaction with Mononucleotides in Solution. In order to confirm that sapphyrin binds nucleotides *via* "phosphate chelation" in solution as well as the solid state, solution ^{31}P NMR studies of various cyclic 3′−5′ monophosphate nucleotides were conducted.[21] These cyclic nucleotide species, by virtue of their monoanionic charge, serve as simple model compounds for the more complex polyanionic nucleotide polymers composed of 5′-to-3′ linked monomers. In their acid or sodium salt form, the ^{31}P resonances of these nucleotides in D_2O/MeOH (1:2) fall in the range of −1.1 to −2.6 ppm.[22] Upon the addition of 1 molar equiv of **1**, these same ^{31}P NMR resonances are shifted upfield significantly (i.e., into the −3.3 to −5.7 ppm range). These upfield shifts are consistent with the phosphoros atom of a given nucleotide, in analogy to Figure 2, being located above the plane of **1** and therefore subject to the ring current effects of the large, aromatic sapphyrin macrocycle.

Further insight into the solution-state chemistry of this interaction was obtained using UV−visible spectroscopy. As seen in Figure 6, when a solution of **1** in aqueous, buffered solution (pH 7.0) is titrated with the pyrimidine-containing nucleotides cCMP or cTMP, the Soret-like transition observed at 409 nm decreases and becomes increasingly replaced by a new absorption at 422 nm. Based on the solid-state structure shown in Figure 2 and the solution ^{31}P NMR studies summarized in Table 1, this new species (i.e. the one that yields the absorption band at 422 nm) is assigned to a phosphate-containing "chelate complex" of the sapphyrin dimer. This critical conclusion is based on the above-mentioned spectroscopic analysis which has led to the characteristic absorption band at 422 nm being assigned to the self-dimerized form of sapphyrin. It is also consistent with other findings made in the context of the present study (*vide infra*).

When UV−visible spectroscopic titrations identical to the above were conducted using **1** and cAMP or cGMP, spectroscopic changes were observed that were far more complex than those seen with either cCMP or cTMP. In the case of cAMP and cGMP (see Figure 7), at low phosphate ester-to-sapphyrin ratios (P/S), the initial band at 409 nm is gradually replaced by one at 422 nm, assigned to the phosphate-bound nucleotide complex of **1**. However, distinct from what happens with the pyrimidine-based cyclic nucleotides, at high P/S ratios the 422-nm band was replaced by a third band at *ca.* 450 nm. This band is assigned to the monomeric form of the nucleotide-bound sapphyrin, in accord with the above-mentioned spectroscopic

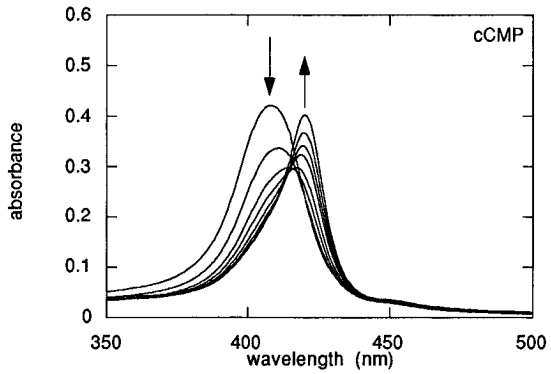

Figure 6. Overlay of the visible spectra of 3 μM sapphyrin **1** in the presence of increasing concentrations of cCMP (P/S ratios of approximately 0, 300, 1000, 2000, 3500, 4800, 6300, and 8300) in 5 mM PIPES, pH 7.0. A titration using cTMP yields a similar result. The redshifted band that grows in at *ca.* 422 nm is assigned to phosphate-bound complex between the dimer of **1** and these nucleotides analogous to the solid-state structure shown in Figure 2. Note the lack of any significant absorbance at *ca.* 450 nm.

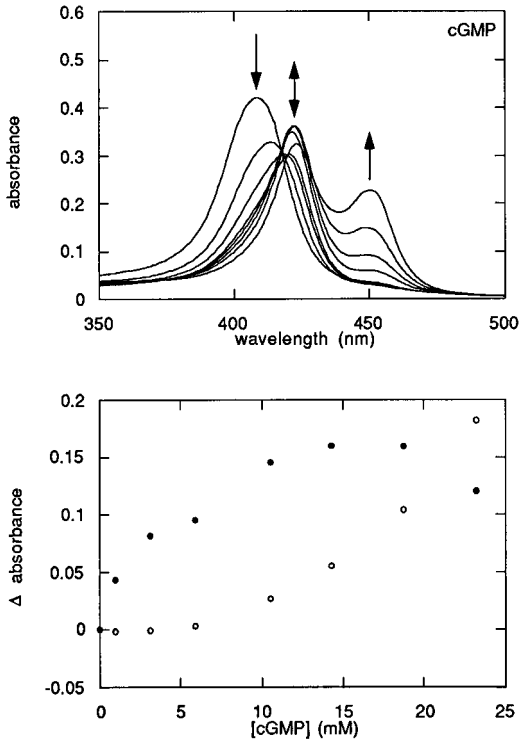

Figure 7. Overlay of the visible spectra of 3 μM sapphyrin **1** in the presence of increasing concentrations of cGMP (P/S ratios of approximately 0, 300, 1000, 2000, 3500, 4800, 6300, and 8300) in 5 mM PIPES, pH 7.0. A titration using cAMP yields a similar result. The absorption band at *ca.* 450 nm is assigned to the monomeric form of **1**. The double arrow indicates the growth and subsequent decay of the indicated absorption band throughout the titration. Shown also are plots of the absorbance at *ca.* 450 (●) and *ca.* 422 nm (○) for **1** as a function of each respective nucleotide.

(20) The titrations were conducted in 10 mM bis-Tris buffer at pH 6.1. Details of the titration and curve-fitting procedures can be found in the supporting information.

(21) Because of problems with precipitation in the concentration regime required for these experiments, the analogous solution phase ^{31}P NMR studies could not be conducted with nucleic acids.

(22) It was necessary to use an organic cosolvent in these studies to avoid problems involving the coprecipitation of sapphyrin and these nucleotides in aqueous solution in the millimolar concentration regime needed for the NMR work.

Table 1. ^{31}P NMR and UV−Visible Spectroscopic Data for Sapphyrin **1** in the Presence of the Indicated Mononucleotide

mononucleotide	δ^a (ppm)	δ^b (ppm)	$\lambda_{max}{}^c$ (nm)	$\lambda_{max}{}^d$ (nm)
cAMP	−2.1 (H^+)	−5.7	423	453
cCMP	−2.3 (H^+)	−5.2	422	no[e]
cGMP	−1.1 (Na^+)	−3.3	422	454
cTMP	−2.6 (Na^+)	−5.4	421	no[e]

[a] ^{31}P NMR chemical shift of the phosphate species recorded as the free acid (H^+) or sodium salt (Na^+) (5 mM) in D_2O/MeOH (1:2) at 298 K. [b] ^{31}P NMR chemical shift of the phosphate species recorded in the presence of 1 molar equivalent of sapphyrin **1**; other conditions as in footnote *a*. [c] λ_{max} of the absorption band (of **1**) assigned to the phosphate-bound complex between the dimer of **1** and the indicated nucleotide species (50 mM) in 5 mM aqueous PIPES buffer, pH 7.0. [d] λ_{max} of the absorption band (of **1**) assigned to the π-stacked complex between the monomeric form of **1** and the indicated nucleotide (50 mM) in 5 mM aqueous PIPES, pH 7.0. [e] n.o. = none observed.

analyses; these have served to show that the monomeric form of sapphyrin exhibits a characteristic absorption at *ca.* 450 nm. The extent of augmentation as a function of concentration for this third band was particularly pronounced in the case of cGMP.

Significantly, no correlation, or proportionality, in relative intensity was found for the two absorption bands that were seen to grow in as a function of increasing nucleotide concentration (Figure 7). This is consistent with the proposal that the absorption bands represent two distinct modes of binding. As indicated in Table 1, the bands assigned to the phosphate-bound complex of the dimer of **1** generally display a fixed, "generic" wavelength of 422 ± 1 nm and similar shapes. By contrast, the bands centered at *ca.* 450 nm have considerably more variability. In addition, the extent to which these latter bands grow in as a function of added cAMP, cGMP, cCMP, and cTMP was also highly variable. In summary, the spectroscopic signature associated with the band at *ca.* 450 nm is one that is highly diagnostic for the particular nucleobase under consideration.

The interaction characterized by the absorption at *ca.* 450 nm is assigned to the monomeric form of sapphyrin π-stacked with a nucleobase. Consistent with this proposal is the finding that a growing in of this band is seen only in the case of the two purine derivatives cAMP and cGMP; only these large heteroaromatic bases offer the possibility for appreciable π-stacking. Further, this proposed interaction, or at least the spectroscopic signature assigned to it, is only observed at high P/S ratios where the sapphyrin macrocycle is more deaggregated through "phosphate chelation". The proposed π-stacking process is thus expected to compete more easily with various sapphyrin self-stacking interactions.

Stacking interactions similar to those discussed above have also been observed in the case of tetrakis(4-*N*-methylpyridyl)-porphine (H_2TMpyP) in the presence of various nucleotides.[23] As in the case of **1**, the magnitude of the interaction of the monomeric form of H_2TMpyP was shown to be dependent on the structure of the nucleotide. Unfortunately, H_2TMpyP is not a good "control" for β-alkyl-substituted sapphyrin **1**. Thus, porphyrin **4** was prepared and studied in the presence and absence of the same four nucleotides considered in the case of **1**. While porphyrin **4** is "water-soluble", it is not monomeric. As evidenced from its spectrum in 5 mM PIPES, pH 7.0 (supporting information), the broad and split nature of the low-intensity Soret absorption of **4** indicates that it is highly aggregated.[24] In the presence of a large excess of nucleotide

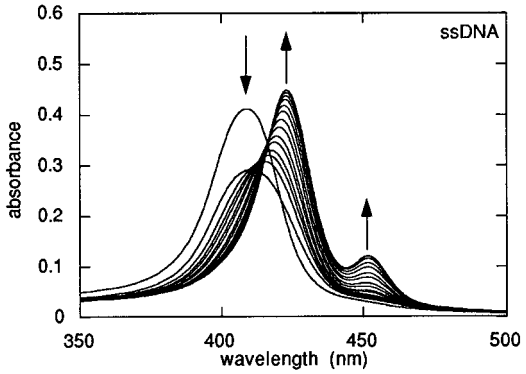

Figure 8. Overlay of the visible spectra of 3 μM sapphyrin **1** recorded in the presence of increasing concentrations of ssDNA−phosphate (from P/S = 0 to 200) in 5 mM PIPES, pH 7.0. Notice the similar pattern of growth for the absorption bands at *ca.* 422 and *ca.* 450 nm as seen in Figure 7.

(e.g., 50 mM), this split Soret absorption, to varying degrees, is replaced by an absorption band centered at *ca.* 400 nm. When **4** is immersed in a 0.1% solution of SDS, conditions that are known to effect the monomerization of aggregated, water-soluble porphyrins[25] (and sapphyrins; *vide supra*), an absorption band at 398 nm appears that resembles that seen with various nucleotides. These results support the suggestion that hydrophobic interactions between nucleotides and large, aromatic macrocycles result not only in complexation but also a concomitant monomerization of the latter.

Interactions with Polynucleotides. As the next logical step in the course of our investigations, interactions between sapphyrin **1** and single-stranded calf thymus DNA (ssDNA) were analyzed. Essentially, this polymer is composed of a heterogeneous mixture of the four 5′-monophosphate deoxyribonucleotides (dAMP, dCMP, TMP, and dGMP) linked in a 5′-to-3′ fashion. Like its constituent monomers, ssDNA has oxyanions, but these are now arranged along an anionic phosphodiester "backbone" and adjacent to the various hydrophobic nucleobases. To a first approximation, therefore, one might expect the interactions of this polynucleotide with **1** to resemble those seen in the case of its constituent monomers. In fact, this proved to be the case.

Shown in Figure 8 are the visible spectra generated when sapphyrin **1** is titrated with ssDNA. As with the simpler mononucleotides, the initial absorption band at 409 nm gives way at relatively low P/S ratios to one that is centered at 422 nm. At higher P/S ratios, this new band gradually gives way to a third band centered at 452 nm. From a phenomenological perspective, the interaction between ssDNA and its nucleotide monomers appears to be very similar. This leads us to conclude that the underlying mode of interaction, to a first approximation, is the same in both instances.

In the case of ssDNA, the apparent λ_{max} for **1** redshifts incrementally to 422 nm as a function of added ssDNA−phosphate (see supporting information). Using this change in the apparent λ_{max} as an indicator of the state of aggregation of **1**, it becomes clear that "phosphate chelation" results in the deaggregation of **1** as this species becomes bound, presumably, along the anionic, phosphodiester backbone of ssDNA. The end point of the titration results in a species with an absorption at 422 nm assigned to the dimeric form of **1**, in accord with the spectroscopic analyses described above.

(23) Pasternack, R. F.; Gibbs, E. J.; Gaudemer, A.; Antebi, A.; Bassner, S.; De Poy, L.; Turner, D. H.; Williams, A.; Laplace, F.; Lansard, M. H.; Merienne, C.; Perrée-Fauvet, M. *J. Am. Chem. Soc.* **1985**, *107*, 8179−8186.

(24) Fuhrhop, J.-H.; Demoulin, C.; Boettcher, C.; Köning, J.; Siggel, U. *J. Am. Chem. Soc.* **1992**, *114*, 4159−4165.

(25) White, W. I. In *The Porphyrins*; Dolphin, D., Ed; Academic Press: New York, 1978; Vol. 5, p 334.

Steady-state fluorescence spectroscopy was used to probe further the sapphyrin−ssDNA interaction. Previous work has shown that deaggregation results in an increase in the steady-state emission yield of the sapphyrin macrocycle.[13,26] Consistent with this model, sapphyrin **1** is found, for all practical purposes, to be non-emissive in solution. This indicates that the macrocycle is significantly aggregated under the aqueous, buffered conditions of this study. However, upon the addition of ssDNA, the steady state emission is observed to increase as a function of added ssDNA−phosphate (see supporting information). Thus, as with the change in the apparent λ_{max}, the observed enhancement of emission would seem to indicate that the highly aggregated form of sapphyrin **1** has become deaggregated along the backbone of ssDNA. This deaggregation, we propose, occurs to form a species wherein the sapphyrin is chelated *as a dimer* to the phosphorylated ssDNA backbone. Support for this conclusion comes from the observation of the critical "marker" absorption at 422 nm; this band, as discussed above, is considered characteristic of this species. In any event, this "thinning out" can be rationalized, as with the simple mononucleotides, to be the result of "phosphate chelation" to the oxyanion backbone of ssDNA, a process that competes with the self-stacking tendency in solution and on the nucleic acid polymer.

During the growth of the 422-nm band, a third band grows in at 452 nm. As in the case of the nucleotides, this absorption band is assigned to monomeric sapphyrin species complexed to the various nucleobases present in ssDNA. This mode of binding could be considered a kind of "pseudointercalation" wherein sapphyrin is bound among or between exposed nucleobases and excluded from the aqueous milieu. While the exact nature of this interaction with the nucleobases of ssDNA is not clear, such a "pseudointercalation" model is not unreasonable. Certain DNA-binding molecules, such as proflavine[27] and H_2-TMpyP,[28] have been proposed to bind to the single-stranded copolymer, poly(deoxyadenylic acid), *via* a "pseudointercalation" mode.

Because of spectroscopic complexities caused by the highly aggregated state of **1** in aqueous solution, as well as the presence of multiple equilibria, association constants for binding to ssDNA could not be derived. Nevertheless, it is important to note that significantly lower per phosphate concentrations of ssDNA−phosphate were required, as compared to various mononucleotides, to effect similar changes in the visible spectrum of **1**. No significant changes in the absorption band at 422 nm in the visible spectrum of **1** take place beyond a P/S ratio of 200 for ssDNA. By contrast, for compounds such as cCMP and cTMP, there are still large increases in the absorbance at 422 nm at P/S ratios greater than 10 000. A reasonable interpretation of these findings is that **1** exhibits a higher affinity for ssDNA than for the individual nucleotides.[29]

Next, the interactions between sapphyrin **1** and double-stranded calf thymus DNA (dsDNA) were examined. This heteropolymer differs from ssDNA in that its highly structured, double-helical nature effectively occludes the nucleobases from the aqueous medium. Indeed, the hydrophobic events that drive this process are to a large degree responsible for maintaining its classic double-helical nature. Finer structural organization, in turn, is governed by nucleobase composition.[30] Significantly, the only major structural feature, from a simple perspective, that dsDNA has in common with ssDNA is an anionic phosphodiester backbone exposed to the aqueous environment.

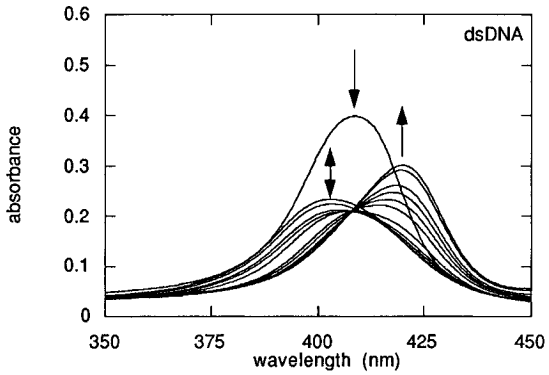

Figure 9. Overlay UV−visible absorption spectra for a 3 μM aqueous solution of sapphyrin **1** in the presence of increasing concentrations of dsDNA−phosphate (from P/S = 0 to 200) in 5 mM PIPES, pH 7.0. The initial absorption at 409 nm (P/S = 0) gives way to a new blueshifted absorption band at 400 nm at a P/S ratio of 1. With additional dsDNA−phosphate, the apparent λ_{max} redshifts to yield an absorption centered at ca. 422 nm at a P/S ratio of 200. The double arrow indicates the growth and subsequent decay of the indicated absorption band throughout the titration.

When **1** was titrated with dsDNA, instead of a redshift being observed for the apparent λ_{max} (as seen with ssDNA), an initial blueshift of 9 nm was seen (see supporting information) that was accompanied by a significant hypochromism in the absorption at *ca.* 400 nm relative to the absorption at 409 nm (see Figure 9). This blueshift is maximal at the point where approximately 1 equiv of dsDNA−phosphate has been added. Upon addition of further equivalents of dsDNA−phosphate, the apparent λ_{max} begins to redshift slowly. As seen in Figure 9, after the addition of 1 equiv of dsDNA−phosphate, the apparent λ_{max} is a composite of two bands, one centered at 400 nm and another at *ca.* 422 nm. This observation leads to the conclusion that there are two distinct interactions of **1** with dsDNA. One of these binding modes, the mode that gives rise to the absorption at 400 nm, is not observed when **1** is titrated with the various prototypical mononucleotides or ssDNA.

Both visible and circular dichroism (CD) spectroscopy were used to ascertain more precisely the nature of the species absorbing at *ca.* 400 nm. The blueshifted nature of this absorption band, in conjunction with the extreme hypochromicity that it exhibits, supports the contention that this species is composed of highly aggregated, stacked sapphyrin macrocycles.[31] Consistent with this conclusion is the finding that sapphyrin **1**, which is achiral, exhibits no CD spectrum alone in solution but at relatively low P/S ratios of dsDNA displays a large conservative (or bisignate) CD spectrum with minima and maxima at 400 and 416 nm, respectively (see supporting information). This latter result also serves to indicate that the species that gives rise to the 400 nm absorption band is highly ordered. Consequently, we conclude that sapphyrin **1**, which is already partially aggregated under these aqueous conditions, is templated into a highly-ordered and chiral aggregate structure associated with the helical backbone of dsDNA.[32] The ob-

(26) Sessler, J. L.; Cyr, M. J.; Maiya, B. G.; Judy, M. L.; Newman, J. T.; Skiles, H. L.; Boriak, R.; Matthews, J. L. *SPIE Int. Opt. Eng.* **1990**, *1203*, 233−245.

(27) Dourlent, M.; Hogrel, J. F. *Biopolymers* **1976**, *15*, 29−41.

(28) Pasternack, R. F.; Brigandi, R. A.; Abrams, M. J.; Williams, A. P.; Gibbs, E. J. *Inorg. Chem.* **1990**, *29*, 4483−4486.

(29) The higher apparent affinity for ssDNA (as opposed to simple phosphates) may reflect the fact that once **1** is complexed to the polyanionic backbone of ssDNA, it is bound to a two-dimensional array of phosphodiester anions. Consequently, because of the high effective concentration of anions present, **1** may have a considerably slower off rate than when bound to a nucleotide monomer in solution.

(30) Saenger, W. *Principles of Nucleic Acid Structure*; Springer-Verlag: New York, 1984.

(31) Cantor, C. R.; Schimmel, P. R. *Biophysical Chemistry. Part II: Techniques for the Study of Biological Structure and Function*; W. H. Freeman and Company: New York, 1980; pp 390−404.

served, induced CD of this species results from the long-range coupling of the transition dipoles of stacked sapphyrin macrocycles which have been induced to orient in some ordered fashion by virtue of interacting with the chiral, double-stranded DNA backbone.

This phenomenon, as well as its rationale, is not unique to this sapphyrin-based system. Similar conservative CD spectra have been observed with acridine orange[33] and various cationic porphyrins, such as *meso*-tetrakis(*p*-*N*-trimethylanilinium)porphine (TMAP),[34] *trans*-bis(4-*N*-methylpyridyl)diphenylporphine,[35] and *meso*-tetrakis[4-[(3-(trimethylamino)propyl)oxy]-phenyl]porphine,[36] in the presence of double-stranded DNA. In these cases, the bisignate, induced CD spectra were found to be the result of a highly organized state of the bound chromophore that was formed in direct response to the helical structure of DNA.

In direct competition with this ordered, aggregated, binding mode is "phosphate chelation". The addition of >1 equiv of dsDNA−phosphate results in the redshift of the apparent λ_{max} of **1** (see supporting information). At roughly 200 equiv of dsDNA−phosphate, this apparent λ_{max} is centered at 420 nm and continues to shift incrementally with additional dsDNA−phosphate equivalents. The low absorbance associated with this latter band suggests an "incomplete" conversion to the phosphate-bound dimer state at this P/S ratio. By contrast, at the same P/S ratio of ssDNA−phosphate, this absorption band assigned to the dimer is both sharp and intense. For dsDNA, this result likely reflects the fact that the competitive templating effect seen at low P/S ratios of dsDNA still exhibits considerable influence at higher P/S ratios.

In addition to the above, fluorescence spectroscopy was also used as a means of probing the nature of the interactions between **1** and dsDNA. When the integrated steady-state emission of a fixed concentration of **1** is plotted as a function of the P/S ratio of dsDNA (see supporting information), behavior is observed that differs considerably in comparison to what is seen when **1** is titrated with ssDNA. In the case of ssDNA, there is a gradual increase in the integrated steady-state emission as a function of added ssDNA−phosphate. In the case of dsDNA, there is a sharp initial rise in the integrated steady-state emission up to a P/S ratio of 1. When additional equivalents of dsDNA−phosphate are added, there is an initial decrease that is followed by a slow and steady rise in the integrated steady-state emission. Based on the concomitant change in the visible and CD spectra, the initial sharp rise in the emission intensity up to P/S ratio of 1 in the presence of dsDNA results from an ordered aggregate mode of binding between **1** and dsDNA. Interestingly, this species is more emissive than the aggregate form of **1** in solution, possibly a consequence of the highly ordered nature of this mode of binding. When additional equivalents of dsDNA-phosphate are added, this species disappears and gives way to a phosphate-bound dimer complex, as indicated by the observation of the diagnostic absorption band at 422 nm. This latter complex, because of the deaggregation of **1** that results, gradually becomes more emissive and results in an increase in the integrated steady-state emission.

In the presence of dsDNA, the porphyrin species **4** exhibits significantly different spectroscopic behavior than **1**. In the presence of a large excess of dsDNA−phosphate there is a slight decrease in the overall intensity of the visible spectrum of **4** (supporting information). In the presence of dsDNA, over a range of P/S ratios, there is no induced CD spectrum associated with **4**. Finally, when **4** is titrated with dsDNA there is a decrease in the integrated steady-state emission intensity (data not shown). Based on the observed hypochromicity and the decreased emission yield, these data, taken together, would seem to indicate that **4** is more aggregated in the presence of dsDNA.[37]

Because of the affinity of sapphyrin for nucleobases, some discussion is required as to whether or not sapphyrin intercalates into dsDNA. Three pieces of evidence argue against the ability of sapphyrin to intercalate: First, we previously demonstrated[8] that **1** does not unwind the double-stranded supercoiled DNA plasmid pBR322 using a topoisomerase I-based assay to detect DNA unwinding, a classic signature of intercalation. Second, no significant absorption band at *ca.* 450 nm for **1** is observed in the presence of dsDNA.[38] This strongly implies, from a spectroscopic viewpoint, that there is no monomeric form, as would be expected upon intercalation of **1** in the presence of dsDNA. Finally, a viscometric analysis has been carried out. This kind of analysis provides a measure of the viscosity of a solution of linear DNA in the presence of a putative intercalator. If the species intercalates and/or unwinds the DNA, the length, and concomitantly the viscosity, of the linear DNA increases. If no intercalation takes place, no significant increase in the viscosity of the DNA is observed. The viscosity data are quantified by plotting the reduced intrinsic viscosity as a function of the ratio of the putative intercalator to DNA base pairs: If the molecule of interest intercalates into DNA, the slope of the resulting line falls between 0.5 and 1.0. If not, the value is near 0.[39] When the known intercalator ethidium bromide was used as a positive control in our assay, the value of the slope was found to be 0.5. When **1** was used, this value was found to be −0.04. This result, in full agreement with the topoisomerase I experiment, indicates that **1** does not unwind double-stranded DNA. Consequently, sapphyrin cannot intercalate into dsDNA.

This lack of intercalation can be rationalized on steric grounds. Based on modeling studies, both the large macrocyclic nature of sapphyrin and the organic "spaghetti" around its periphery prohibit **1** from fitting between a given set of base pairs without considerably disrupting surrounding base-pairing motifs. In the case of known intercalators, such as ethidium bromide, their smaller size and unadorned periphery are more easily accommodated between the base pairs of double-stranded DNA. Steric arguments have also been used to explain the inability of certain axial-ligated, metalated versions of H_2TMpyP to intercalate into double-stranded DNA.[40] In the case of these cationic porphyrins, the combined steric *thickness* of the metalated H_2TMpyP and its axial ligand was used as the

(32) Tinoco, I.; Woody, R. W.; Bradley, D. F. *J. Chem. Phys.* **1963**, *38*, 1317−1325.

(33) Blake, A.; Peacocke, A. R. *Biopolymers* **1966**, *4*, 1091−1104.

(34) Carvlin, M. J.; Datta-Gupta, N.; Fiel, R. J. *Biochem. Biophys. Res. Commun.* **1982**, *108*, 66−73.

(35) (a) Gibbs, E. J.; Tinoco, I., Jr.; Maestre, M. F.; Ellinas, P. A.; Pasternack, R. F. *Biochem. Biophys. Res. Commun.* **1988**, *157*, 350−358. (b) Pasternack, R. F.; Giannetto, A. *J. Am. Chem. Soc.* **1991**, *113*, 7799−7800.

(36) Marzilli, L. G.; Pethö, G.; Lin, M.; Kim, M. S.; Dixon, D. W. *J. Am. Chem. Soc.* **1992**, *114*, 7575−7577.

(37) Slama-Schwok, A.; Lehn, J.-M. *Biochemistry* **1990**, *29*, 7895−7903.

(38) In some cases, a small absorption band resembling that seen with ssDNA was seen at *ca.* 450 nm at very high P/S ratios (>300) of dsDNA. The appearance of this band was found to be dependent on the batch of dsDNA used and likely reflects the fact that double-stranded calf thymus DNA inevitably contains trace amounts of unpaired single strands. As a result, there is likely some hydrophobic interaction, as discussed in the case of ssDNA, with exposed nucleobases.

(39) (a) Jones, R. L.; Davidson, M. W.; Wilson, W. D. *Biochim. Biophys. Acta* **1979**, *561*, 77−84. (b) Wakelin, L. P. G. *Med. Res. Rev.* **1986**, *6*, 275−340.

(40) (a) Pasternack, R. F.; Gibbs, E. J.; Villafranca, J. J. *Biochemistry* **1983**, *22*, 2406−2414. (b) Gibbs, E. J.; Maurer, M. C.; Zhang, J. H.; Reiff, W. M.; Hill, D. T.; Malicka-Blaszkiewicz, M.; McKinnie, R. E.; Liu, H-Q.; Pasternack, R. J. *J. Inorg. Biochem.* **1988**, *32*, 39−65.

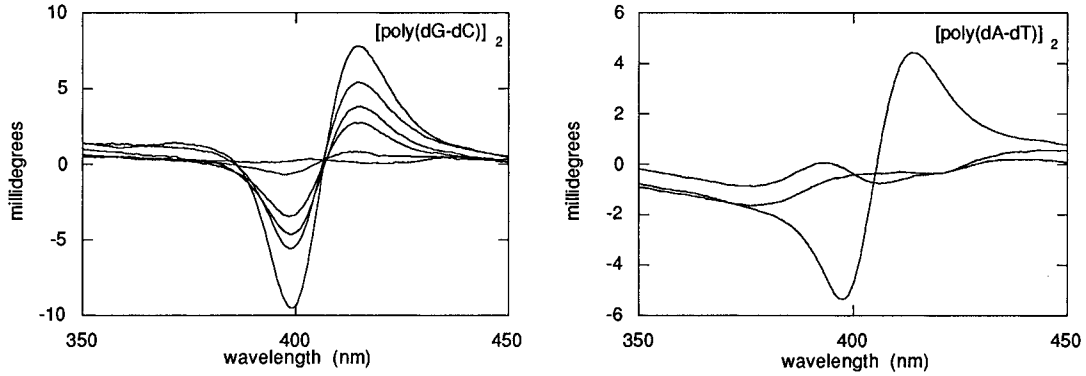

Figure 10. Induced CD spectra of sapphyrin **1** in the visible region recorded in the presence of $[poly(dG\text{-}dC)]_2$ and $[poly(dA\text{-}dT)]_2$ in 5 mM PIPES, pH 7.0. Spectra for the former copolymer are shown in order of decreasing intensity at P/S ratios of 1, 10, 20, 40, 80, and 140. Spectra for the latter copolymer are shown in order of decreasing intensity at P/S ratios of 1, 5, and 10.

rationale for the inability of these species to intercalate. In the case of sapphyrin, other factors, such as the location of the positive charge and the ability of "phosphate chelation" to compete efficiently with an intercalative mode, may also come into play.

In order to investigate what sequence or structural specificity might be associated with the interactions between **1** and dsDNA, experiments involving the synthetic, double-stranded copolymers $[poly(dA\text{-}dT)]_2$ and $[poly(dG\text{-}dC)]_2$ were carried out. When **1** was titrated with each of these copolymers, the resulting complexes exhibited certain spectroscopic features similar to those seen with dsDNA. At a P/S ratio equal to 1 for each copolymer, the resulting visible spectra of **1** displayed strong absorbances at 400 nm that were accompanied by the appearance of a conservative induced CD signal for the sapphyrin chromophore. These CD signals exhibited minima and maxima at 399 and 414 nm, respectively. These values closely resemble those gleaned from the conservative CD spectrum seen for **1** in the presence of low P/S ratios of heterogenous dsDNA. As a result, we conclude both helical copolymers are capable of inducing the same ordered aggregate binding mode for **1** as is observed in the presence of dsDNA.

While there were similarities in the spectroscopic behavior of **1** in the presence of these copolymers, there were also dramatic differences. In each case, the addition of >1 equiv of DNA−phosphate resulted in a redshift in the apparent λ_{max} of **1** and the appearance of a band at *ca.* 422 nm. As in the case of dsDNA, this band is considered indicative of the fact that sapphyrin **1** is chelated to the phosphodiester backbone in its dimeric form. In the case of $[poly(dA\text{-}dT)]_2$, considerably less DNA−phosphate was required to effect the same augmentation in this absorption band than in the case of $[poly(dG\text{-}dC)]_2$. Correspondingly, the conservative induced CD signal that accompanies the band at 400 nm disappears more rapidly upon the addition of $[poly(dA\text{-}dT)]_2$ versus $[poly(dG\text{-}dC)]_2$ (see Figure 10). As a result, we conclude the "phosphate chelation" mode of binding is favored in the case of $[poly(dA\text{-}dT)]_2$ relative to $[poly(dG\text{-}dC)]_2$.

While a preference for $[poly(dA\text{-}dT)]_2$ over $[poly(dG\text{-}dC)]_2$, has been found to be the result of favorable minor groove binding interactions for molecules known to undergo this mode of DNA binding,[41] we do not favor groove binding as being the dominant form of interaction with dsDNA for **1**. In the case of both ssDNA and dsDNA at high P/S ratios of DNA−phosphate, a strong absorption at 422 nm appears, clearly indicative of the dimer. Because ssDNA lacks a well-defined groove, it thus follows that groove binding is unlikely to be a dominant mode for the binding for **1** with dsDNA.

Instead, we would rationalize the preference of **1** for $[poly(dA\text{-}dT)]_2$ as being the result of the more flexible nature inherent in $[poly(dA\text{-}dT)]_2$ as compared to $[poly(dG\text{-}dC)]_2$. AT-rich areas of dsDNA, by virtue of the two-point Watson and Crick type hydrogen bonding motif between adenine and thymine are known to be more susceptible to "localized melting" than GC-rich areas.[42] Consistent with this known behavior, $[poly(dA\text{-}dT)]_2$, when modeled as a uniform, elastic rod, has been shown to be less rigid than its GC counterpart, $[poly(dG\text{-}dC)]_2$.[43] Thus, $[poly(dA\text{-}dT)]_2$ is likely to be more adaptable, from a steric perspective, to a DNA binding mode analogous to the solid-state structure seen in Figure 2. Because of the nature of binding in the context of dsDNA, the particulars of "phosphate chelation" are expected to be sensitive to steric demands imposed by localized, structural microenvironments of dsDNA. $[Poly(dA\text{-}dT)]_2$, by virtue of its greater flexibility, would likely be more accommodating toward **1** as compared to its more rigid and less flexible $[poly(dG\text{-}dC)]_2$ analogue.[44]

Conclusion

The interaction of the water-soluble sapphyrin derivative **1** with a variety of nucleic acids has been described. Three modes of interaction have been demonstrated. The first mode, seen with all nucleotide and nucleic acid species, is that of "phosphate chelation". This mode is exemplified by a solid-state structure made up of the monobasic form of cAMP and the sapphyrin species $[2H\cdot\mathbf{2}]^{2+}$. Spectroscopically, this interaction is characterized by a visible absorption at 422 nm for the dimeric form of **1** complexed to phosphorylated nucleotides. In the case of double-stranded DNA, the "phosphate chelation" mode of binding shows a preference for the more flexible copolymer $[poly(dA\text{-}dT)]_2$ over $[poly(dG\text{-}dC)]_2$. The second mode involves a hydrophobic interaction with the nucleobases present in both monomeric and single-stranded polymeric nucleotides. Spectroscopically, this nucleotide-dependent interaction is character-

(41) Fairley, T. A.; Tidwell, R. R.; Donkor, I.; Naiman, N. A.; Ohemeng, K. A.; Lombardy, R. J.; Bentley, J. A.; Cory, M. *J. Med. Chem.* **1993**, *36*, 1746−1753.

(42) (a) Early, T. A.; Kearns, D. R.; Hilen, W.; Wells, R. D. *Biochemistry* **1981**, *20*, 3756−3764. (b) Early, T. A.; Kearns, D. R.; Hilen, W.; Wells, R. D. *Biochemistry* **1981**, *20*, 3756−3764.

(43) Milar, D. P.; Robbins, R. J.; Zewail, A. H. *J. Chem. Phys.* **1981**, *74*, 4200−4201.

(44) While groove binding could not be rigorously ruled out, similar electrostatic arguments were employed to explain the high degree of selectivity for $[poly(dA\text{-}dT)]_2$ over $[poly(dG\text{-}dC)]_2$ seen for certain cationic porphyrins containing peripherally attached methylated pyridinium cations, see: (a) Strickland, J. A.; Marzilli, L. G.; Gay, K. M.; Wilson, W. D. *Biochemistry* **1988**, *27*, 8870−8878. (b) Lin, M.; Lee, M.; Yue, K. T.; Marzilli, L. G. *Inorg. Chem.* **1993**, *32*, 3217−3226. (c) Mukundan, N. E.; Pethö, G.; Dixon, D. W.; Marzilli, L. G. *Inorg. Chem.* **1995**, *34*, 3677−3687.

ized by the absorption of the monomeric species of **1** at *ca.* 450 nm. The third mode involves the highly ordered aggregation of **1** on the surface of certain double-stranded, helical nucleic acids at low P/S ratios and is templated by the higher order structure of these nucleic acid polymers. Spectroscopically, this mode is characterized by a visible absorption at 400 nm and a large, conservative induced CD signal for **1**. In general, the data are not consistent with **1** binding to dsDNA *via* either groove-binding or intercalation.

Further studies of the interactions between **1** and dsDNA might allow the recognition aspects of the binding processes to be better detailed and the specificity of the interaction, if any, to be more fully revealed. Toward this end, affinity cleavage studies[45] with a recently synthesized sapphyrin−EDTA conjugate[46] and HPLC separations of oligonucleotides using sapphyrin-modified silica gels[6c] are being made; these are designed to elucidate the nature of any putative sequence or structural selectivity that could arise as the result of "phosphate chelation". In addition, we are exploring the use of "phosphate chelation" as a type of "anchor" in the design of novel antisense strategies.[47,48] Here, the goals are to augment the normal intocell uptake rates associated with oligonucleotide fragments and to enhance the intrastrand binding constant for antisense agents to complementary nucleic acid species.

Acknowledgment. We would like to thank Dr. Anthony Harriman for his helpful comments. This work was supported by an NSF-PYI award (CHE-9157440) to B. L. I. and by NIH Grant No. AI 33577 to J.L.S. Partial support from Pharmacyclics, Inc. (to J.L.S.) and the Howard Hughes Medical Institute (to J.L.S. and V.K.) is also gratefully acknowledged.

Supporting Information Available: Figures, tables, and text giving summaries of further optical analyses, viscosity studies, binding constant determination methods, and full analysis of the X-ray diffraction data for $[2H\cdot\mathbf{2}]^{2+}\cdot cAMP^{-}\cdot Cl^{-}$ (53 pages). This material is contained in many libraries on microfiche, immediately follows this article in the microfilm version of the journal, can be ordered from the ACS, and can be downloaded from the Internet; see any current masthead page for ordering information and Internet access instructions.

JA952961X

(45) Dervan, P. B. *Science* **1986**, *283*, 464−471.
(46) Iverson, B. L.; Shreder, K.; Morishima, T.; Rosingana, M.; Sessler, J. L *J. Org. Chem.* **1995**, *60*, 6616−6620.
(47) Kabanov, A. V.; Kabanov, V. A. *Bioconj. Chem.* **1995**, *6*, 7−20.
(48) Uhlmann, E.; Peyman, A. *Chem. Rev.* **1990**, *90*, 453−584.